



Numerical Schemes for Fractional Energy Balance Model of Climate Change with Diffusion Effects

Muhammad Shoaib Arif ^{1*}, Kamaleldin Abodayeh ¹, Yasir Nawaz ²

¹ Department of Mathematics and Sciences, College of Humanities and Sciences, Prince Sultan University, Riyadh, 11586, Saudi Arabia.

² Department of Mathematics, Air University, PAF Complex E-9, Islamabad 44000, Pakistan.

Abstract

This study aims to propose numerical schemes for fractional time discretization of partial differential equations (PDEs). The scheme is comprised of two stages. Using von Neumann stability analysis, we ensure the robustness of the scheme. The energy balance model for climate change is modified by adding source terms. The local stability analysis of the model is presented. Also, the fractional model in the form of PDEs with the effect of diffusion is given and solved by applying the proposed scheme. The proposed scheme is compared with the existing scheme, which shows a faster convergence of the presented scheme than the existing one. The effects of feedback, deep ocean heat uptake, and heat source parameters on global mean surface and deep ocean temperatures are displayed in graphs. The current study is cemented by the fact-based popular approximations of the surveys and modeling techniques, which have been the focus of several researchers for thousands of years.

Mathematics Subject Classification: 65P99, 86Axx, 35Fxx.

Keywords:

Numerical Scheme;
Energy Balance Model;
Finite Difference Method;
Diffusion Effect; Stability.

Article History:

Received:	08	November	2022
Revised:	28	February	2023
Accepted:	06	March	2023
Available online:	03	May	2023

1- Introduction

Today, climate change is a widespread terminology used by literary society to make people aware of the hazardous effects and drastic changes produced by it. Fluctuations like elevated temperatures, changed seasonal horizons, long summers, and short winters are among those that affect human beings and microorganisms. These changes increased the struggling rate of organisms to ensure their survival; however, variations in the ecosystem along the riverside are extremely drastic because the average temperature change rate along coastal lines is more than that of the estimated 0.3°C. According to one given report, massive industrialization and anthropogenic perturbation have raised the earth's temperature by 0.3°C, which is beyond the carrying capacity of an ecosystem. The net bearing capacity of the ecosystem for high temperatures is 4°C, which could be achieved by the end of the 21st century. A devastating threat to humankind is the climatic change that has gravitated to the attention of philanthropists and government personnel regarding its preventive measures [1, 2]. The major cause of this change is the burning of fossil fuels, which raises the level of greenhouse gases and increases the chance of global warming [3, 4]. Earth behaving like a volcano could initiate irreversible changes in its chemical, physical, and biological properties, resulting in non-linear, abrupt, and irreparable damage [5, 6].

Water expands when it gets warmer due to the earth's high temperature, which causes its expansion. An Intergovernmental Panel on Climate Change (IPCC) in the United Nations from 1993 to 2003 revealed that each year

* **CONTACT:** marif@psu.edu.sa

DOI: <http://dx.doi.org/10.28991/ESJ-2023-07-03-011>

© 2023 by the authors. Licensee ESJ, Italy. This is an open access article under the terms and conditions of the Creative Commons Attribution (CC-BY) license (<https://creativecommons.org/licenses/by/4.0/>).

about a 3 mm rise in sea level has been observed, and half of this rise is due to the expansion of water by heat [1]. The rise in the earth's temperature is expected to cause an energy imbalance because it absorbs more solar radiation than it emits thermal radiation. In this regard, greenhouse gases play a significant role by forming a thick layer around the atmosphere and preventing thermal radiation's movement across it [7]. Global warming increases the earth's temperature and increases the likelihood of volcanic eruptions, heat stroke, and severe radiation disproportion. Therefore, the consequences of global warming go beyond merely raising the temperature [8].

A luxuriant and mechanical lifestyle followed by clearing land for residential purposes has added more CO₂ to the atmosphere. As a result, the whole earth acted as glass and raised the chances of becoming a greenhouse. This greenhouse gas formed an additional layer across the earth's surface and hindered the sun's rays from escaping it, increasing the temperature globally and leading to heatstroke or a heatwave [9–11]. These temperature variations affect aquatic life and their movements, as evident from the shifted records of phytoplankton towards the North Sea. In contrast, this migration has changed the oceanic weather poleward [12, 13]. The motion of phytoplankton from the Atlantic to the cold water of green land has been variable so far; therefore, the ecologist and weather investigators collectively worked to control the migration and weather shift. In this regard, mathematicians have offered their services to calculate the mass change of phytoplankton through modeling and provide a suitable solution to prevent their extinction due to an unfavorable environment [14–20].

Later on, modern and fractional calculus have taken over the traditional one and can effectively elaborate on the present, past, and future [21–25]. These studies revealed the practical conversion of real-world problems through the differential equation, which describes the whole density and spectrum lying between two integer orders. Modern and non-local fractional-order derivatives have ruled over conventional-order derivatives in fractional calculus. Firstly, Riemann and Liouville have proposed the first-ever definition of a fractional order derivative [26]. Secondly, Caputo modified the conventional derivative by introducing a local singular kernel named the Caputo derivative. After that, in 2015, Caputo and Fabrizio further studied and manipulated this derivative by replacing the singular kernel, i.e., including the Mittag-Leffler, which is non-singular [27]. Finally, in 2016, further modification of the Caputo and Fabrizio derivatives was done by building non-local and non-singular kernels by adding the Mittag-Leffler function [28]. Nowadays, this fractional derivative has its worth in solving real-world problems [29, 30]. The Caputo derivative has the unique characteristic of having a single kernel. It grows at both ends of the transmission spectrum and exhibits a cross-over pattern for the amplitude of its mean square. This property enables the modeling of competition among living species for their survival. Climate change and pandemics can be modeled [31, 32].

A second-order numerical approximation for Caputo-Fabrizio fractional derivative has been given in Liu et al. [33] at node $t_{k+\frac{1}{2}}$. It was mentioned $O(M^2)$ operations and $O(M)$ Stages were required for the non-local property of the Caputo-Fabrizio, where the number of divided intervals was denoted by M . Another fast algorithm based on a novel approximation technique was developed, which consumed $O(M)$ operations and $O(1)$ for memory stages. Another numerical approach, the local discontinuous Galerkin method [34], was employed with a new Caputo-Fabrizio fractional derivative for solving fractal mobile/immobile transport equations. The stability of the local discontinuous Galerkin method was proved, and prior error estimates were also derived.

The current study will provide great insight into preventing climatic change by using Caputo's fractional derivative, which is more efficient than the traditional integer model. The energy balance model is modified using the source term of the non-linear type. Also, the effect of the diffusion term describes the spread of temperature over the spatial variable. The partial differential equation version is more flexible than the standard model. The proposed scheme is capable of solving the modified model. The scheme is finite difference discretization for the temporal term in the parabolic equation. Results are supported through numerical simulation.

Predicting the climate system's evolution in response to natural and human-caused perturbations is impossible without resorting to mathematical models and numerical methods. Different types of mathematical models and numerical methods have played an important role for several decades. In Soldatenko et al. [35], for studying the earth's climate change, some methods and mathematical models were presented with the use of sensitivity analysis. The variation of climate was studied using stochastic models, and essential features of this modeling have been discussed. The application of a low-order energy balance model was explored for studying variations in climate. The influences of variations in feedback and the climate system's inertia were estimated using the sensitivity analysis approach. A simple radiative balance climate model has been presented in North [36] that includes constant homogeneous cloudiness, zonal averaging, an ice feedback mechanism, and ordinary diffusive thermal heat transfer. The simplest model with one parameter was solved analytically, and the solution was found in hypergeometric functions. The ice sheet latitude in terms of the solar constant was studied using this solution. It was proved that the presented climate and ice-covered earth were stable, which was done by stability analysis of the equilibrium solutions.

Mathematical modeling of the earth's climate is a powerful tool for studying climate variations in the future. Mathematical models construct sophisticated models in which a dynamical system represents the simulated processes and ordinary or partial differential equations are used to describe them. There are four climate models: a simple climate

model, a general circulation model of the atmosphere based on sea ice and the upper mixed ocean layer, an intermediate complexity model, and a fully coupled atmosphere-ocean general circulation model. For accurate and reliable results, complex models can be proposed. Based on some factors, a suitable climate model can be chosen. Among the mathematical models of climate change, the energy balance model (EBM) is quite effective and simple. Budyko [37] and Sellers [38] introduced these models about 50 years ago.

The model equations for the energy balance model are expressed as:

$$C \left(\frac{dT}{dt} \right) = -\lambda T - \gamma(T - T_D) + F \quad (1)$$

$$C_D \left(\frac{dT_D}{dt} \right) = \gamma(T - T_D) \quad (2)$$

where T denotes the global mean surface temperature and T_D shows global mean ocean temperature, C represents the heat capacity of the upper box, which is consisted of oceanic and atmosphere surface mixed layer; λ represents the climate feedback parameter which is a proportionality coefficient between the global mean surface temperature (GMST) and radiative response, C_D represents the effective heat capacity of the deep ocean, γ is used for the deep-ocean heat uptake parameter, and F is the forcing term.

Since Equations 1 and 2 are ordinary differential equations that only use the information of time variables, classical ordinary time derivatives are also used in these equations, which are replaced by a more general fractional derivative with the diffusive spatial term. The diffusive term is used to describe the diffusion temperature over a spatial variable. The proposed fractional model can be expressed as:

$$C \left(\frac{\partial^\alpha T}{\partial t^\alpha} \right) = d_1 \left(\frac{\partial^2 T}{\partial x^2} \right) - \lambda T - \gamma(T - T_D) + QT^2 \quad (3)$$

$$C_D \left(\frac{\partial^\alpha T_D}{\partial t^\alpha} \right) = d_2 \left(\frac{\partial^2 T_D}{\partial x^2} \right) + \gamma(T - T_D) \quad (4)$$

where $0 < \alpha \leq 1$ & d_1 & d_2 are diffusion coefficients.

Equations 3 and 4 are fractional partial differential equations having diffusive terms and a source term in Equation 3. At this stage, a local stability analysis for the corresponding ordinary differential equations is presented for Equations 3 and 4 using $d_1 = 0 = d_2$.

To find the equilibrium points, set

$$0 = -\lambda T - \gamma(T - T_D) + QT^2 \quad (5)$$

$$0 = \gamma(T - T_D) \quad (6)$$

Solving Equations 5 and 6 give the following points of equilibrium:

$$B_0(0,0), \quad B_1 \left(\frac{\lambda}{Q}, \frac{\lambda}{Q} \right)$$

where T and T_D denotes, respectively first and second coordinates in B_0 and B_1 .

Since Equations 5 and 6 are non-linear, their Jacobin, if found, is expressed as:

$$J = \begin{vmatrix} -\lambda - \gamma + 2QT & \gamma \\ \gamma & -\gamma \end{vmatrix} \quad (7)$$

At the equilibrium point B_1 The Jacobin can be expressed as:

$$J|_{B_1} = \begin{vmatrix} \lambda - \gamma & \gamma \\ \gamma & -\gamma \end{vmatrix} \quad (8)$$

The characteristic polynomial $R(y)$ can be expressed as:

$$R(y) = y^2 + (2\gamma - \lambda)y - \gamma\lambda \quad (9)$$

where y denotes the eigenvalues of $J|_{B_1}$. For the system to be a stable eigenvalue of $J|_{B_1}$ should be non-negative. To impose the condition of getting negative eigen values, the Routh Hurwitz criterion will be applied. According to this criterion for second-degree polynomials, the coefficients of y and the constant term of $R(y)$ must be negative. Therefore,

$$2\gamma - \lambda < 0 \quad \text{and} \quad -\gamma\lambda < 0 \quad (9)$$

Since the constant term in Equation 9 is already negative, so the condition of getting a negative eigenvalue is $\lambda < 2\gamma$. So, when this mentioned condition is satisfied, the system of Equations 3 and 4 using $d_1 = 0 = d_2$ will be stable. Equations 3 and 4 will be solved numerically using a numerical fractional scheme.

Basic Concepts:

Before starting the working procedure of numerical schemes for fractional differential equations, some basic literature related to the fractional derivative is given.

Definition: The Caputo fractional derivative is defined as [39]:

$$D_t^\alpha V(t) = \frac{1}{\Gamma(\alpha-m)} \int_0^t \frac{v^m(\tau) d\tau}{(t-\tau)^{\alpha-m+1}}, \text{ where } m-1 < \alpha \leq m$$

Definition: For a function v , the fractional integral operator is defined as:

$$I_c^\alpha f(y) = \frac{1}{\Gamma(\alpha)} \int_a^y (y-t)^{\alpha-1} f(t) dt$$

Lemma: If $m-1 < \alpha \leq m$, then the following properties hold:

$$(1) D_t^\alpha I_c^\alpha v(t) = v(t)$$

$$(2) (I_c^\alpha D_t^\alpha)v(t) = v(t) - \sum_{k=0}^{m-1} v^{(k)}(0^+) \frac{t^k}{k!}$$

Since the numerical scheme for the fractional differential equation is already given in Soldatenko et al. [35], the approximation is also considered in this work for constructing a numerical scheme for solving the fractional differential equation. The numerical approximation for the fractional-order derivative can be derived by employing fractional Taylor series expansion.

$$u_i^{n+1} = u_i^n + \frac{(\Delta t)^\alpha}{\alpha!} \left. \frac{\partial u}{\partial t} \right|_i^n + O((\Delta t)^{2\alpha})$$

This implies

$$\left. \frac{\partial u}{\partial t} \right|_i^n = \frac{\alpha!(u_i^{n+1}-u_i^n)}{(\Delta t)^\alpha} + O((\Delta t)^{2\alpha})$$

2- Construction of Fractional Numerical Scheme

In the initial level of construction, a difference equation with some unknown parameters is constructed. In a later stage, the unknown parameters will be determined. Also, the scheme will be constructed for the system's first Equation 3. The constructing procedure for Equation 4 will be similar.

The scheme is an explicit and implicit type fractional scheme. The first stage of the scheme is explicit, whereas the second stage is implicit. For its first stage, a difference equation for Equation 3 is expressed as:

$$\bar{T}_i^{n+1} = T_i^n + \frac{(\Delta t)^\alpha}{\Gamma(\alpha+1)} (D_t^\alpha T_i^n) \tag{11}$$

This stage (Equation 11) is explicit. For the implicit stage, a difference equation in implicit form is constructed as:

$$T_i^{n+1} = aT_i^n + b\bar{T}_i^{n+1} + \frac{(\Delta t)^\alpha}{\Gamma(\alpha+1)} \{cD_t^\alpha \bar{T}_i^{n+1} + eD_t^\alpha T_i^{n+1} + fD_t^\alpha T_i^n\} \tag{12}$$

where a, b, c, e , and f are unknown parameters determined later. Using fractional Taylor series for T_i^{n+1} and $D_t^\alpha T_i^{n+1}$ as:

$$T_i^{n+1} = T_i^n + \frac{(\Delta t)^\alpha}{\Gamma(\alpha+1)} (D_t^\alpha T_i^n) + \frac{(\Delta t)^{2\alpha}}{\Gamma(2\alpha+1)} (D_t^{2\alpha} T_i^n) + \frac{(\Delta t)^{3\alpha}}{\Gamma(3\alpha+1)} (D_t^{3\alpha} T_i^n) + O((\Delta t)^{4\alpha}) \tag{13}$$

$$D_t^\alpha T_i^{n+1} = D_t^\alpha T_i^n + \frac{(\Delta t)^\alpha}{\Gamma(\alpha+1)} (D_t^{2\alpha} T_i^n) + \frac{(\Delta t)^{2\alpha}}{\Gamma(2\alpha+1)} (D_t^{3\alpha} T_i^n) + O((\Delta t)^{3\alpha}) \tag{14}$$

Substituting Equations 13 and 14 into Equation 12 results:

$$T_i^n + \frac{(\Delta t)^\alpha}{\Gamma(\alpha+1)} (D_t^\alpha T_i^n) + \frac{(\Delta t)^{2\alpha}}{\Gamma(2\alpha+1)} (D_t^{2\alpha} T_i^n) + \frac{(\Delta t)^{3\alpha}}{\Gamma(3\alpha+1)} (D_t^{3\alpha} T_i^n) = aT_i^n + b\bar{T}_i^{n+1} + \frac{(\Delta t)^\alpha}{\Gamma(\alpha+1)} \left\{ cD_t^\alpha \bar{T}_i^{n+1} + e \left(D_t^\alpha T_i^n + \frac{(\Delta t)^\alpha}{\Gamma(\alpha+1)} (D_t^{2\alpha} T_i^n) + \frac{(\Delta t)^{2\alpha}}{\Gamma(2\alpha+1)} (D_t^{3\alpha} T_i^n) \right) + fD_t^\alpha T_i^n \right\} \tag{15}$$

Substituting Equation 11 into Equation 15 and comparing coefficients of $T_i^n, D_t^\alpha T_i^n, D_t^{2\alpha} T_i^n$ and $D_t^{3\alpha} T_i^n$ give the following linear equations:

$$\left. \begin{aligned} 1 &= a + b \\ 1 &= b + c + e + f \\ \frac{(\Delta t)^{2\alpha}}{\Gamma(2\alpha+1)} &= \frac{(\Delta t)^\alpha}{\Gamma(\alpha+1)} \left\{ \frac{c(\Delta t)^\alpha}{\Gamma(\alpha+1)} + \frac{e(\Delta t)^\alpha}{\Gamma(\alpha+1)} \right\} \\ \frac{(\Delta t)^{3\alpha}}{\Gamma(3\alpha+1)} &= \frac{(\Delta t)^\alpha}{\Gamma(\alpha+1)} \frac{e(\Delta t)^{2\alpha}}{\Gamma(2\alpha+1)} \end{aligned} \right\} \tag{16}$$

Solving Equation 16 yields

$$\left. \begin{aligned} b &= 1 - a \\ e &= \frac{\Gamma(\alpha+1)\Gamma(2\alpha+1)}{\Gamma(3\alpha+1)} \\ c &= \frac{(\Gamma(\alpha+1))^2}{\Gamma(2\alpha+1)} - \frac{\Gamma(\alpha+1)\Gamma(2\alpha+1)}{\Gamma(3\alpha+1)} \\ f &= 1 - b - c - e \end{aligned} \right\} \tag{17}$$

The flow chart of the implementation of this scheme is described in Figure 1.

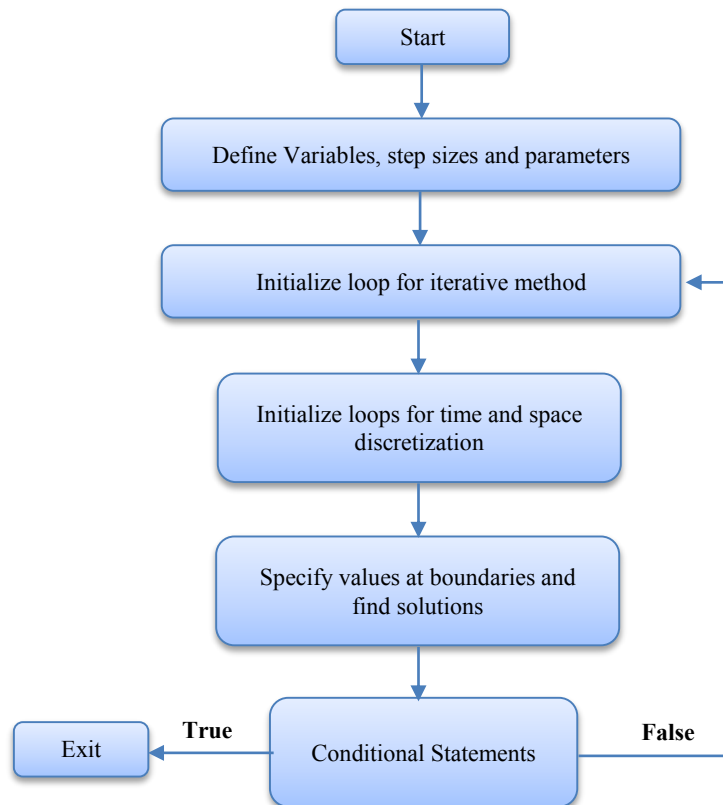


Figure 1. Flow chart of considered algorithm

3- Stability Analysis

A Von Neumann stability criterion is employed to check the stability of the constructed scheme. System of Equations 3 and 4, having only diffusion terms, are expressed as:

$$D_t^\alpha \mathbf{U} = A \frac{\partial^2 \mathbf{U}}{\partial x^2} \tag{18}$$

where $\mathbf{U} = [T, T_D]^T, A = \begin{bmatrix} d_1 & 0 \\ 0 & d_2 \end{bmatrix}$.

Applying the first stage of the constructed scheme on Equation 18 using second-order central difference spatial discretization yields:

$$\bar{\mathbf{U}}_i^{n+1} = \mathbf{U}_i^n + \frac{A(\Delta t)^\alpha}{\Gamma(\alpha+1)} \delta_x^2 \mathbf{U}_i^n \tag{19}$$

Applying the second stage of the constructed scheme to Equation 18 yields:

$$\mathbf{U}_i^{n+1} = a\mathbf{U}_i^n + b\bar{\mathbf{U}}_i^{n+1} + \frac{A(\Delta t)^\alpha}{\Gamma(\alpha+1)} \{c\delta_x^2 \bar{\mathbf{U}}_i^{n+1} + e\delta_x^2 \mathbf{U}_i^{n+1} + f\delta_x^2 \mathbf{U}_i^n\} \tag{20}$$

Consider the following transformations:

$$\left. \begin{aligned} \bar{U}_i^{n+1} &= \bar{E}^{n+1} e^{i\psi}, U_i^{n+1} = E^{n+1} e^{i\psi} \\ U_{i+1}^n &= E^{n+1} e^{(i\pm 1)\psi}, U_{i+1}^{n+1} = E^{n+1} e^{(i\pm 1)\psi} \end{aligned} \right\} \tag{21}$$

Substituting transformations from Equation 21 into Equation 18 and dividing the resulting equation with $e^{i\psi}$ gives:
It will be better to put the values and write the equation here.

$$\bar{E}^{n+1} = E^n + \frac{A(\Delta t)^\alpha}{\Gamma(\alpha+1)} \left\{ \frac{e^{i\psi} - 2 + e^{-i\psi}}{(\Delta x)^2} \right\} E^n \tag{22}$$

Equation 22 is simplified as:

$$\bar{E}^{n+1} = A\{1 + 2d_\alpha(\cos\psi - 1)\}E^n \tag{23}$$

where $d_\alpha = \frac{(\Delta t)^\alpha}{\Gamma(\alpha+1)(\Delta x)^2}$.

Substituting transformation from Equation 21 into Equation 20 and dividing both sides of the resulting equation by $e^{i\psi}$, it yields:

$$E^{n+1} = aE^n + b\bar{E}^{n+1} + \frac{A(\Delta t)^\alpha}{\Gamma(\alpha+1)} \left\{ c\bar{E}^{n+1} \frac{(2\cos\psi - 2)}{(\Delta x)^2} + eE^{n+1} \frac{(2\cos\psi - 2)}{(\Delta x)^2} + f \frac{(2\cos\psi - 2)}{(\Delta x)^2} E^n \right\} \tag{24}$$

Substituting Equation 23 into Equation 24 is obtained:

$$E^{n+1} = aE^n + bA(1 + 2d_\alpha(\cos\psi - 1))E^n + 2d_\alpha A \left\{ \begin{aligned} &A(\cos\psi - 1)(1 + 2d_\alpha(\cos\psi - 1))cE^n + \\ &e(\cos\psi - 1)E^{n+1} + f(\cos\psi - 1)E^n \end{aligned} \right\} \tag{25}$$

Equation 25 is simplified to:

$$\frac{E^{n+1}}{E^n} = (\bar{I} - 2d_\alpha A e(\cos\psi - 1))^{-1} \{ a\bar{I} + bA(1 + 2d_\alpha(\cos\psi - 1)) + 2Ad_\alpha A(\cos\psi - 1)(1 + 2d_\alpha(\cos\psi - 1))c \} + f(\cos\psi - 1) \tag{26}$$

where \bar{I} is an identity matrix of size 2×2 . Let λ_A be the maximum Eigenvalues of A , and then the stability condition is expressed as:

$$\left| \frac{\{a + b\lambda(1 + 2d_\alpha(\cos\psi - 1)) + 2\lambda_A d_\alpha \lambda_A (\cos\psi - 1)(1 + 2d_\alpha(\cos\psi - 1))c\}}{(1 - 2d_\alpha \lambda_A e(\cos\psi - 1))} \right| \leq 1 \tag{27}$$

4- Results and Discussions

The proposed scheme for time discretization is third-order accurate in time according to the Taylor series and second-order accurate in space. Observing the central difference formula's spatial second order can confirm the spatial order. The order of the difference formula can be proved by applying the Taylor series. Also, spatial accuracy can be enhanced by using a higher-order central difference formula for the spatial term. Since the order of the proposed scheme is greater than the first order in space and time, the scheme is consistent according to the considered analysis. Therefore, according to the Lax equivalence theorem, the consistent finite difference scheme will converge if it is stable for linear PDEs. Therefore, the proposed numerical scheme will converge conditionally in the classical case.

The first stage of the proposed scheme is simply the first-order forward Euler scheme that can be capable of finding solutions to fractional non-linear differential equations without linearization. But, the step size should be chosen appropriately so that both stages of the proposed scheme converge. The convergence of the scheme also depends on the chosen values of parameters in the given set of differential equations. Stability is only found for a fractional parabolic equation without having source terms. So, the stability condition does not depend on the source term(s), but it can be extended to fractional time-dependent partial differential equations having source terms. Also, Von Neumann stability can be applied to non-linear PDEs by making them linearized. So, some estimated conditions from linearized PDE can be obtained so that before solving those non-linear equations, the condition on step size can be chosen appropriately. The stability condition also depends on the chosen numerical scheme. The proposed schemes involve more than one parameter, so by choosing the appropriate value of the parameter(s), different numerical schemes can be applied without putting much effort into the computational code. The stability condition may vary for every chosen numerical scheme. Since the proposed scheme is explicit and implicit in two stages, it may require an iterative scheme to solve the difference equation obtained by applying the proposed scheme. So, the solution is found iteratively, and this iterative procedure will stop if the given stopping criterion is met.

Figures 2 to 9 show the results obtained by solving Equations 3 and 4 numerically with some initial and boundary conditions. Figure 2 deliberates the comparison of the proposed scheme with existing numerical schemes. For comparison purposes, one of the existing schemes is backward in time and central in space. This comparison is related to fractional schemes. Since the backward in time and central in space (BTCS) scheme is first order in time, it takes more iterations to converge. The Crank-Nicolson scheme is second-order in space and time, converging faster than

BTCS. The proposed scheme is third-order in fractional time, faster than the other two schemes. Figure 3 shows the impact of climate feedback parameter λ on global mean surface temperature T and global mean deep ocean temperature T_D . The impact of the parameter is shown on both time and space variables. Global mean surface and global mean deep ocean temperatures decrease incrementally in the feedback parameter. Figure 4 shows the impact of deep-ocean heat uptake parameter γ on the global mean surface and ocean temperatures. Both types of temperatures de-escalate by the growth of deep-ocean heat uptake parameters. But the global mean surface temperature has both increasing and decreasing behavior when the heat uptake parameter varies. The impact of heat source parameter Q on the global mean surface and global mean deep ocean temperatures are displayed in Figure 5. Figure 5 shows that global mean surface and global mean deep ocean temperatures escalate by rising heat source parameters. Figures 6 to 9 show the contour plots for global mean surface and deep ocean temperatures.

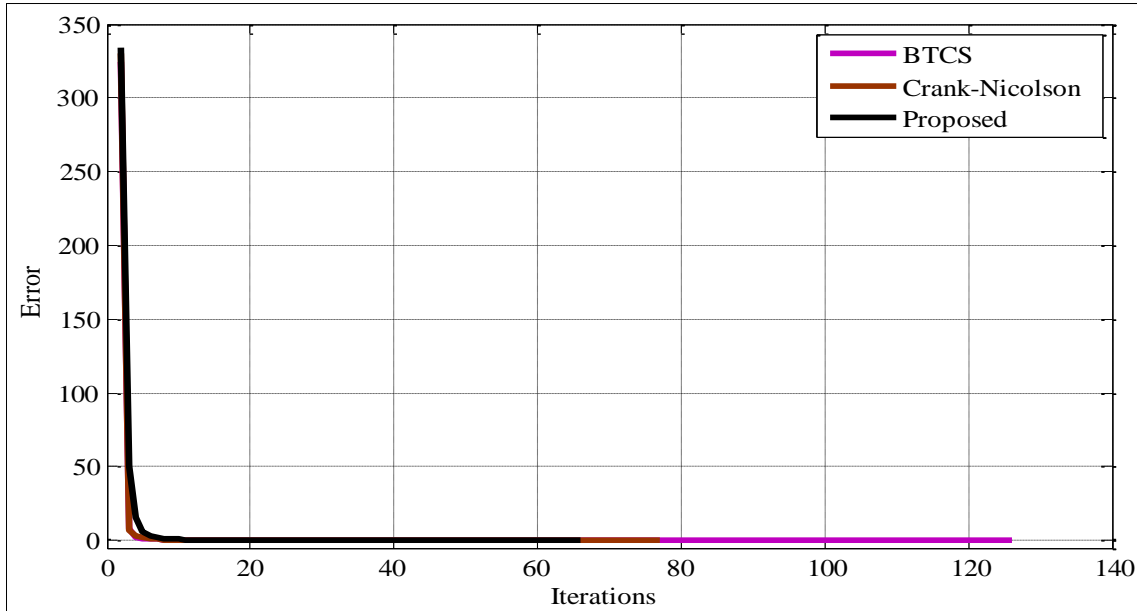


Figure 2. Convergence of three schemes using $\lambda = 0.5, \gamma = 0.1, d_1 = 0.5, d_2 = 0.7, Q = 0.07, a = 0.9, N_x = 50, N_t = 1000, \alpha = 0.95$

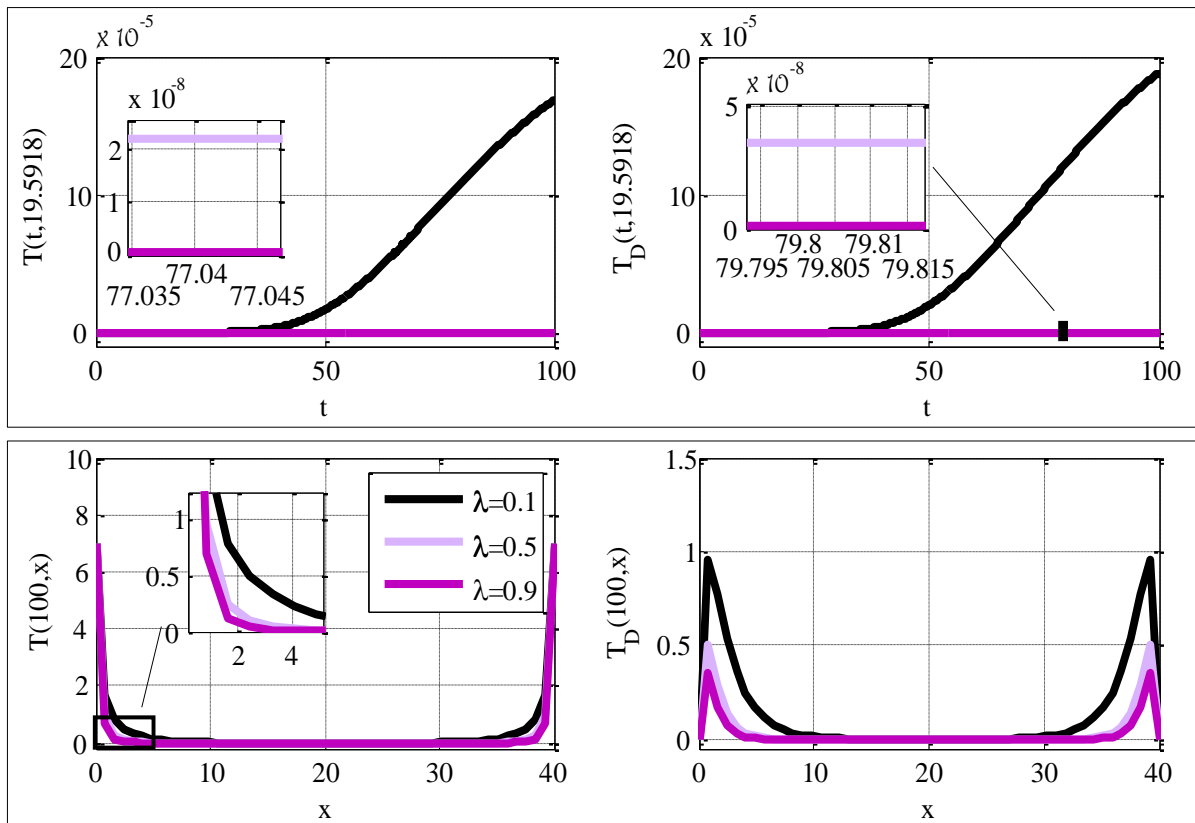


Figure 3. Impact of feedback parameter λ on the global mean surface and deep ocean temperatures using $\gamma = 0.7, d_1 = 0.1, d_2 = 0.3, Q = 0.01, a = 0.7, N_x = 50, N_t = 1000, \alpha = 0.95$

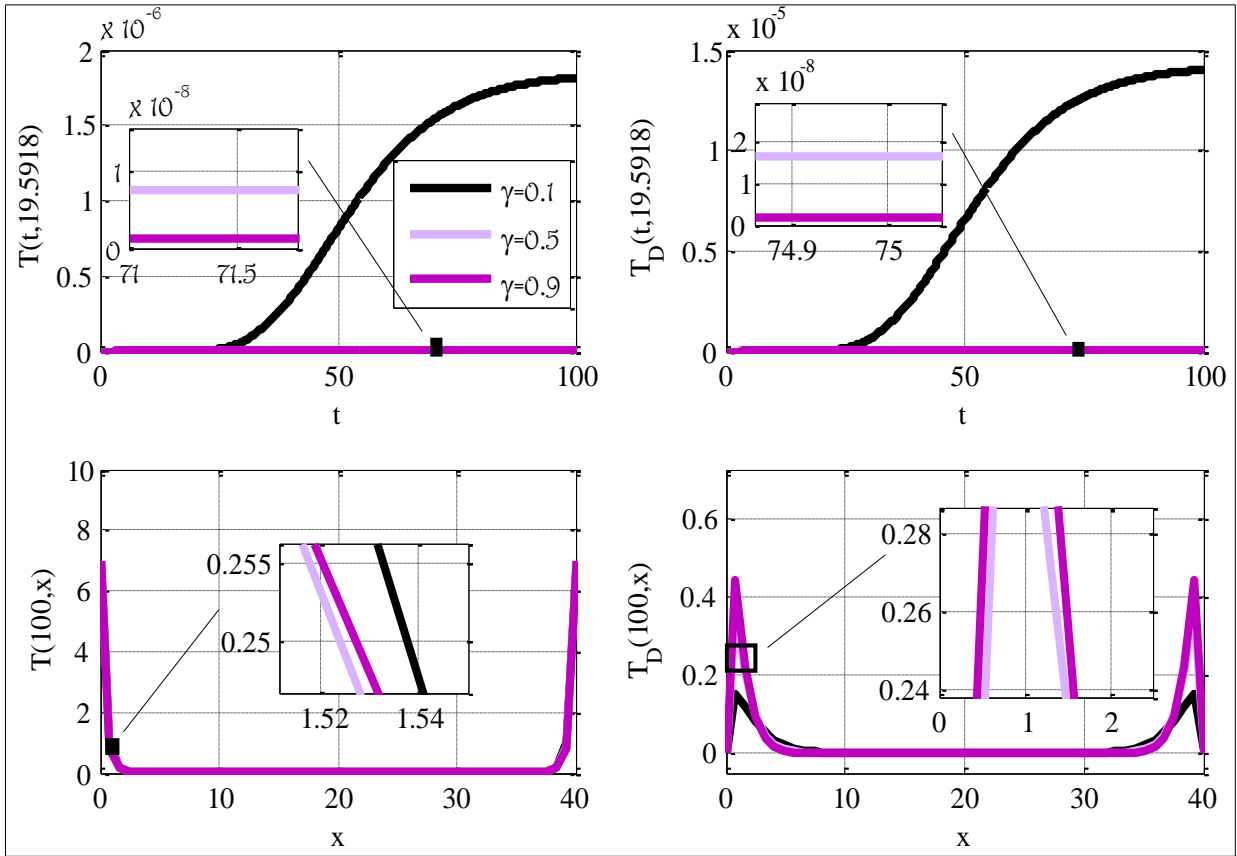


Figure 4. Impact of deep-ocean heat uptake parameter γ on the global mean surface and deep ocean temperatures using $\lambda = 0.7, d_1 = 0.1, d_2 = 0.3, Q = 0.01, a = 0.7, N_x = 50, N_t = 1000, \alpha = 0.95$

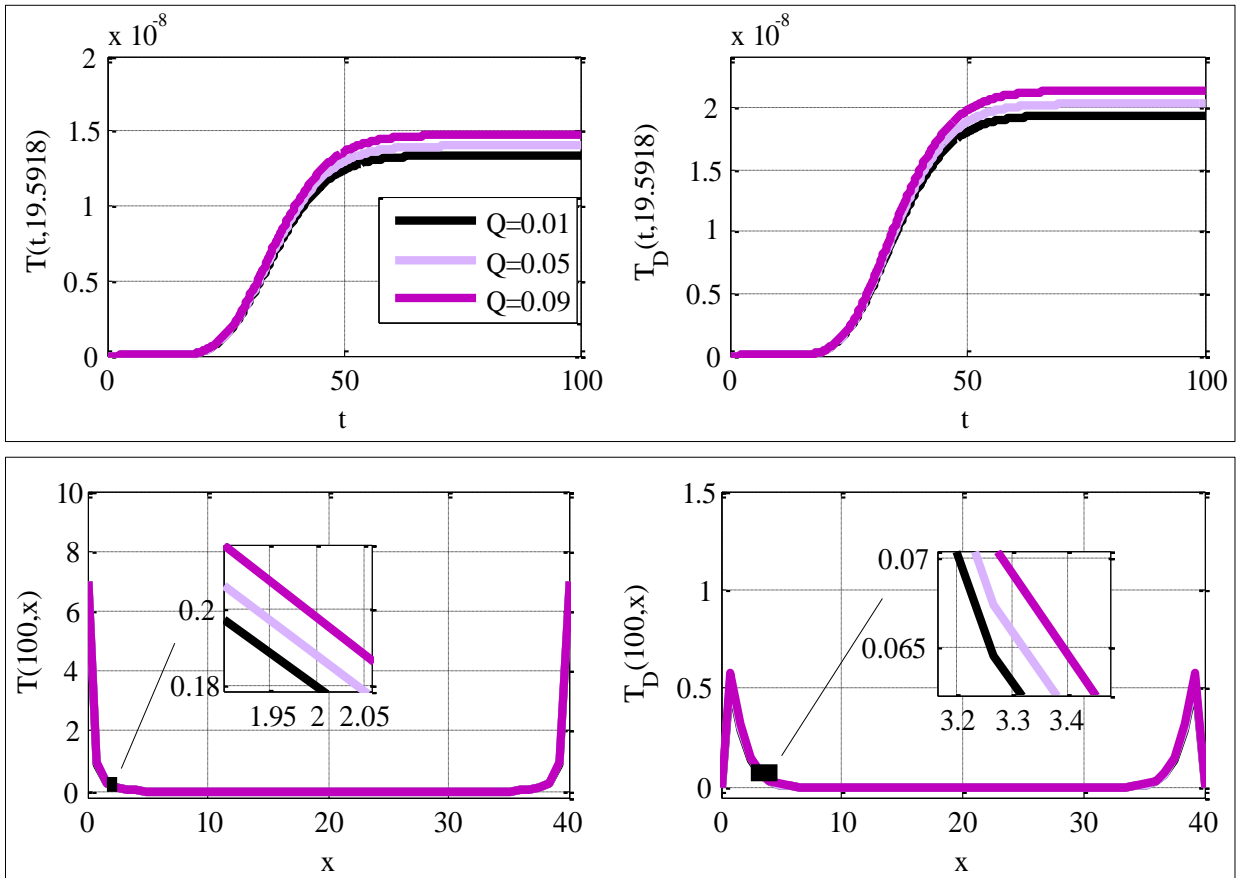


Figure 5. Impact of heat source parameter Q on the global mean surface and deep ocean temperatures using $\lambda = 0.5, d_1 = 0.1, d_2 = 0.3, \gamma = 0.9, a = 0.7, N_x = 50, N_t = 1000, \alpha = 0.95$

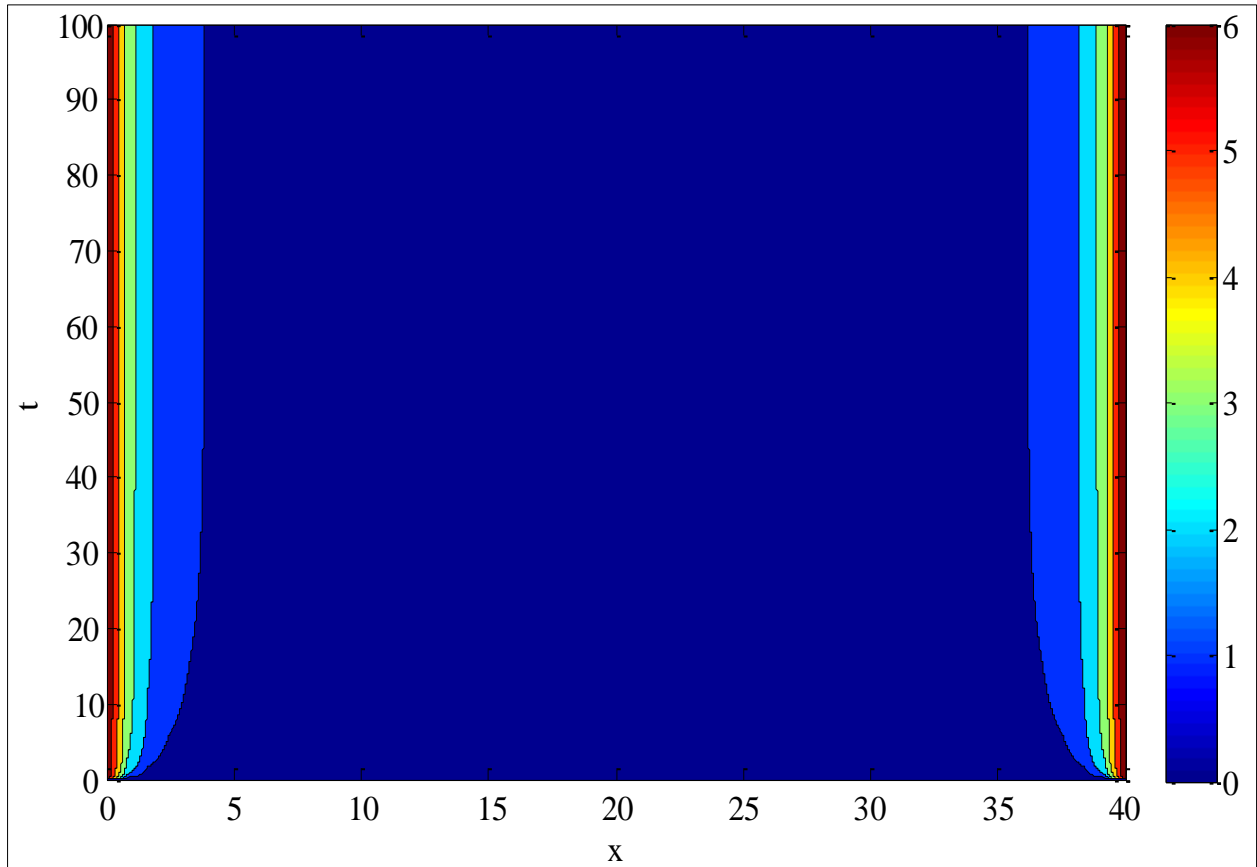


Figure 6. Contours for global mean surface temperature using $\lambda = 0.1, d_1 = 0.5, d_2 = 0.7, \gamma = 0.7, Q = 0.01, a = 0.9, N_x = 50, N_t = 1000, \alpha = 0.95$

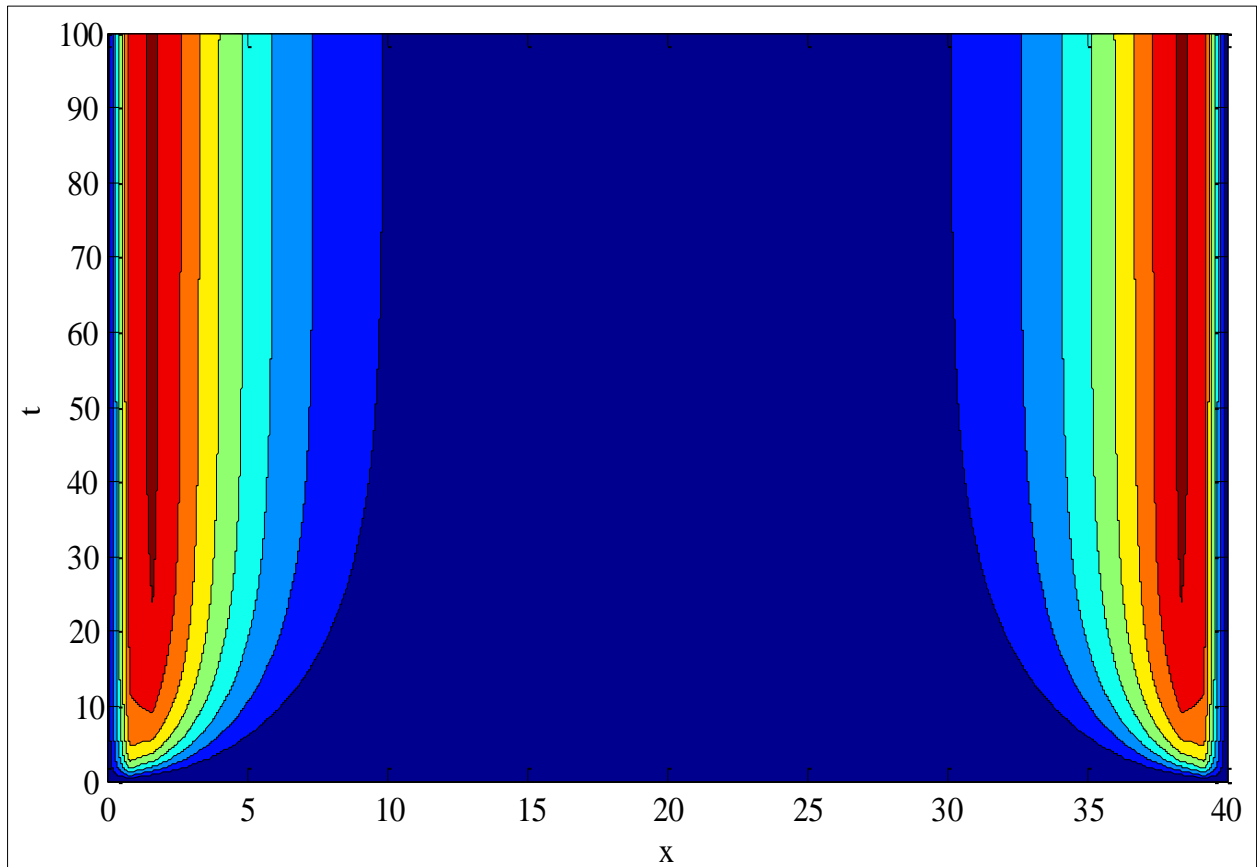


Figure 7. Contours for global mean deep ocean temperature using $\lambda = 0.1, d_1 = 0.5, d_2 = 0.7, \gamma = 0.7, Q = 0.01, a = 0.9, N_x = 50, N_t = 1000, \alpha = 0.95$

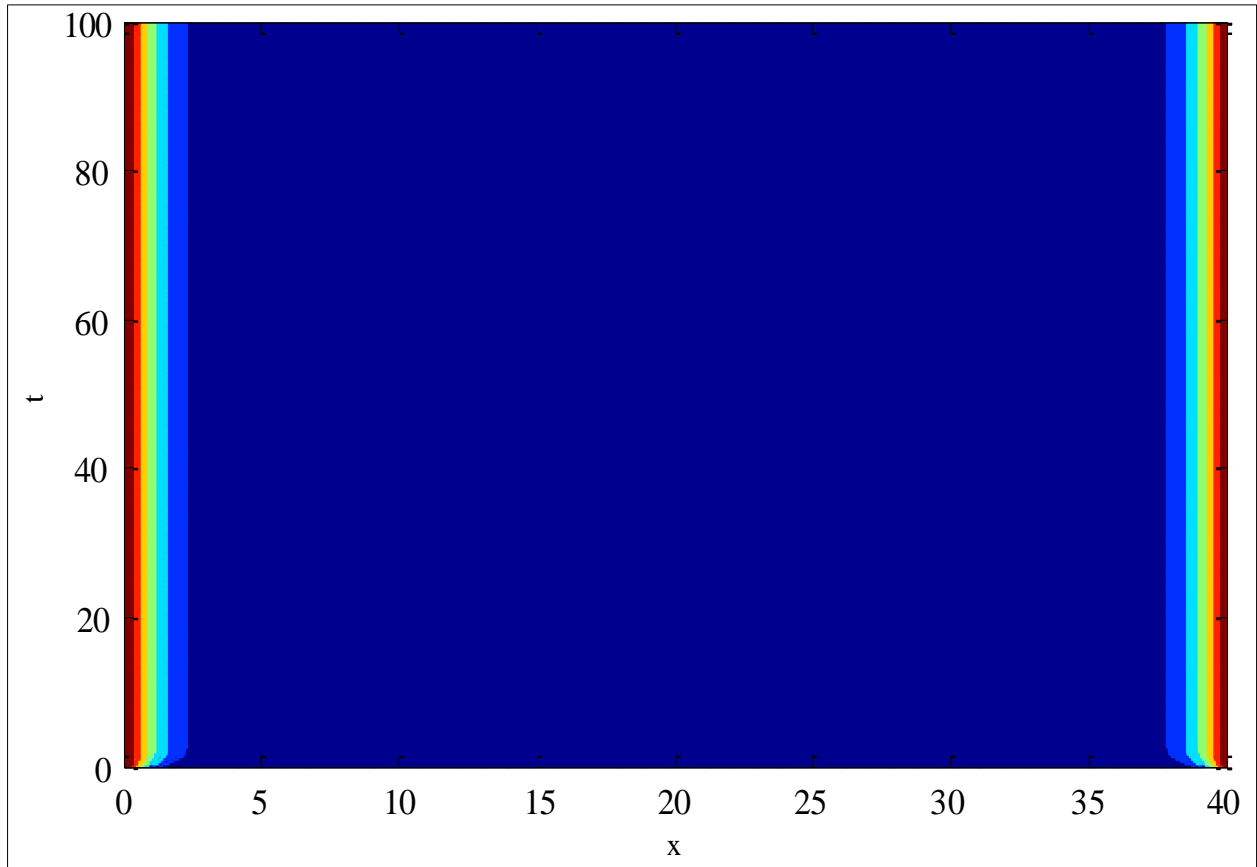


Figure 8. Contours for global mean surface temperature using $\lambda = 0.5, d_1 = 0.5, d_2 = 0.7, \gamma = 0.1, Q = 0.07, a = 0.9, N_x = 50, N_t = 1000, \alpha = 0.7$

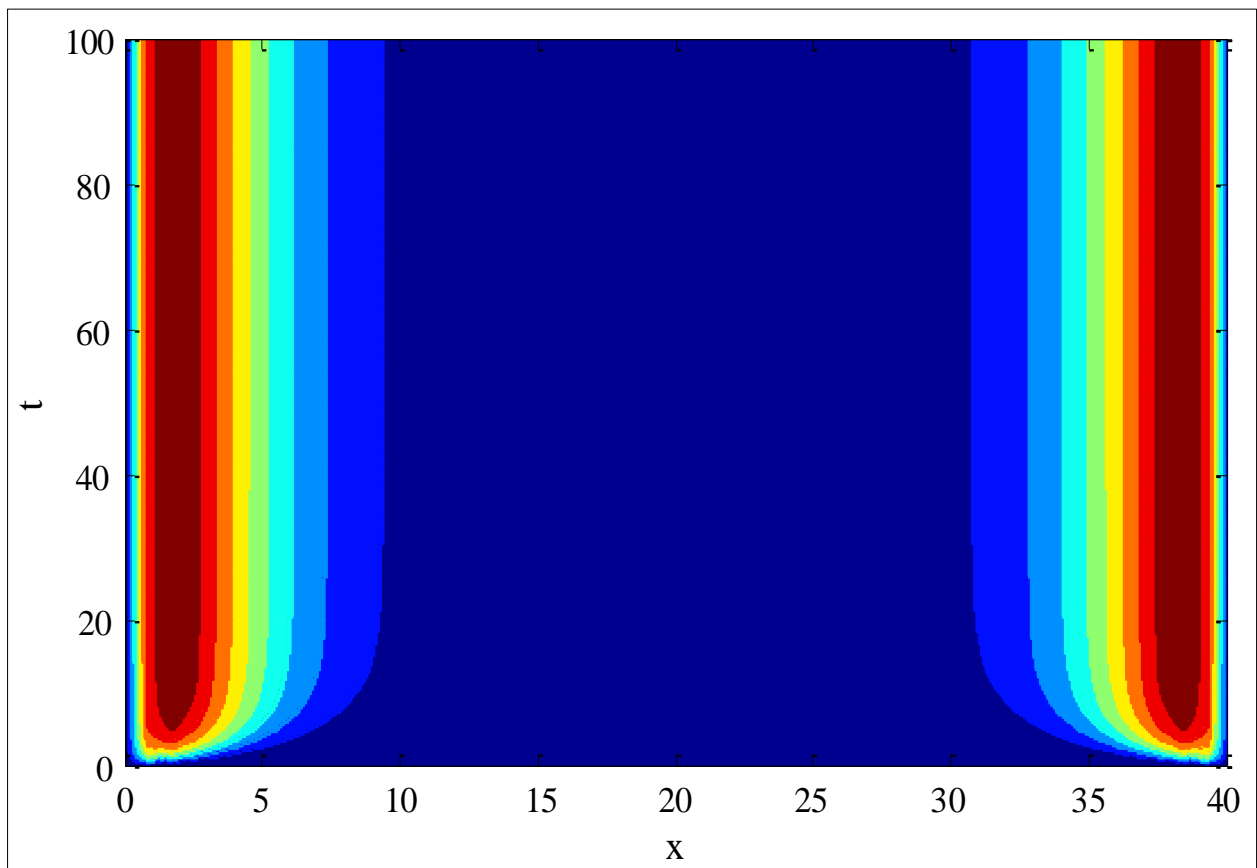


Figure 9. Contours for global mean deep ocean temperature using $\lambda = 0.5, d_1 = 0.5, d_2 = 0.7, \gamma = 0.1, Q = 0.07, a = 0.9, N_x = 50, N_t = 1000, \alpha = 0.7$

Table 1 compares the results obtained by the proposed and existing schemes with the Matlab solver ode45. The trapezoidal scheme is second-order and does not require any restriction on step size to converge. The Matlab solver ode45 is a ready-made code that can solve any scalar or system of linear and non-linear ODEs. This solver uses a high-order numerical scheme to find the solution(s) to the given ODE(s). The difference of numerical solutions obtained by the proposed/existing schemes and Matlab solver ode45 is found, and then the norm of absolute difference is listed in Table 1. Since the numerical solution is considered in place of the exact solution, the norm of error is still reduced by increasing grid points N for the particular case.

Table 1. Comparison of proposed/existing numerical schemes with Matlab solver *ode45* for finding norm of error in global mean surface temperature T using $\alpha = 1$, $\lambda = 0.1$, $\gamma = 0.07$, $Q = 0.01$, $d_1 = d_2 = 0$ and $a = 0.9$, $b = 0.1$

N	$\ ode45 - Trapezoidal\ _2$	$\ ode45 - Proposed\ _2$
100	5.5523×10^{-05}	3.7429×10^{-05}
200	1.9298×10^{-05}	1.3097×10^{-05}
400	6.7137×10^{-06}	4.6717×10^{-06}
800	2.2729×10^{-06}	1.7656×10^{-06}
1600	7.4841×10^{-07}	8.5228×10^{-07}

5- Conclusion

This work was related to proposing a numerical scheme for solving fractional and classical time-dependent partial differential equations. We arrived at a more general and realistic conclusion by employing a fractional mathematical model to simulate climate change. The scheme was third-order accurate, and its order can be observed from its construction procedure. The stability analysis of the scheme was also provided. The effect of the contained parameters on the global mean and surface temperature was shown in the graphs. As a result, we concluded that a fractional version of the model produces a satisfactory equivalent result for climate control. From the obtained results, it was observed that increasing feedback parameters de-escalated global mean surface and deep ocean temperatures, and global mean surface and deep ocean temperatures decayed by increasing deep ocean heat uptake parameters. The proposed numerical scheme can be further applied to epidemiological disease models and other problems [40–43] in fractional calculus.

6- Declarations

6-1- Author Contributions

Conceptualization, M.S.A. and Y.N.; methodology, Y.N.; software, Y.N.; validation, M.S.A., K.A., and M.S.A.; formal analysis, K.A.; investigation, M.S.A.; resources, K.A.; data curation, K.A.; writing—original draft preparation, M.S.A.; writing—review and editing, K.A.; visualization, Y.N.; supervision, M.S.A.; project administration, K.A.; funding acquisition, K.A. All authors have read and agreed to the published version of the manuscript.

6-2- Data Availability Statement

The data presented in this study are available on request from the corresponding author.

6-3- Acknowledgements

The authors wish to express their gratitude to Prince Sultan University for facilitating the publication of this article through the Theoretical and Applied Sciences Lab.

6-4- Institutional Review Board Statement

Not applicable.

6-5- Informed Consent Statement

Not applicable.

6-6- Conflicts of Interest

The authors declare that there is no conflict of interest regarding the publication of this manuscript. In addition, the ethical issues, including plagiarism, informed consent, misconduct, data fabrication and/or falsification, double publication and/or submission, and redundancies have been completely observed by the authors.

7- References

- [1] Solomon, S., Qin, D., Manning, M., Chen, Z., Marquis, M., Averyt, K., Tignor, M., & Miller, H. (2007). IPCC fourth assessment report (AR4). *Climate change 2007: The physical Science Basis*. Cambridge University Press, Cambridge, United Kingdom.
- [2] Watson, R. T. (2001). *Climate Change 2001: Synthesis Report*. Contribution of Working Groups I, II, and III to the Third Assessment Report of the Intergovernmental Panel on Climate Change. IPCC 2001, Cambridge university Press, Cambridge, United Kingdom.
- [3] Aizebeokhai, A. P. (2009). Global warming and climate change: Realities, uncertainties and measures. *International journal of physical sciences*, 4(13), 868-879.
- [4] de Larminat, P. (2016). Earth climate identification vs. anthropic global warming attribution. *Annual Reviews in Control*, 42, 114–125. doi:10.1016/j.arcontrol.2016.09.018.
- [5] Mitchell, A. (2009). *Sea sick: The global ocean in crisis*. McClelland & Stewart Limited, Toronto, Canada.
- [6] Ogotu, B. K. Z. N. (2015). Energy balance mathematical model on climate change. Ph.D. Thesis, Université Pierre ET Marie University of Nairobi, Nairobi, Kenya.
- [7] Pierrehumbert, R. T. (2010). *Principles of planetary climate*. Cambridge University Press, New York, United States. doi:10.1017/CBO9780511780783.
- [8] Masih, A. (2018). An Enhanced Seismic Activity Observed Due To Climate Change: Preliminary Results from Alaska. *IOP Conference Series: Earth and Environmental Science*, 167, 012018. doi:10.1088/1755-1315/167/1/012018.
- [9] Malchow, H., Petrovskii, S. V., & Venturino, E. (2007). *Spatiotemporal patterns in ecology and epidemiology: theory, models, and simulation*. CRC Press, New York, United States. doi:10.1201/9781482286137.
- [10] McCarty, J. P. (2001). Ecological Consequences of Recent Climate Change. *Conservation Biology*, 15(2), 320–331. doi:10.1046/j.1523-1739.2001.015002320.x.
- [11] Jonkers, L., Hillebrand, H., & Kucera, M. (2019). Global change drives modern plankton communities away from the pre-industrial state. *Nature*, 570(7761), 372–375. doi:10.1038/s41586-019-1230-3.
- [12] Rayner, N. A., Parker, D. E., Horton, E. B., Folland, C. K., Alexander, L. V., Rowell, D. P., Kent, E. C., & Kaplan, A. (2003). Global analyses of sea surface temperature, sea ice, and night marine air temperature since the late nineteenth century. *Journal of Geophysical Research: Atmospheres*, 108(D14). doi:10.1029/2002jd002670.
- [13] Poloczanska, E. S., Brown, C. J., Sydeman, W. J., Kiessling, W., Schoeman, D. S., Moore, P. J., Brander, K., Bruno, J. F., Buckley, L. B., Burrows, M. T., Duarte, C. M., Halpern, B. S., Holding, J., Kappel, C. V., O'Connor, M. I., Pandolfi, J. M., Parmesan, C., Schwing, F., Thompson, S. A., & Richardson, A. J. (2013). Global imprint of climate change on marine life. *Nature Climate Change*, 3(10), 919–925. doi:10.1038/nclimate1958.
- [14] Houghton, E. (1996). *Climate change 1995: The science of climate change: contribution of working group I to the second assessment report of the Intergovernmental Panel on Climate Change*. Cambridge University Press, Cambridge, Unite Kingdom.
- [15] Metz, B., Davidson, O., Swart, R., & Pan, J. (2001). *Climate change 2001: mitigation: contribution of Working Group III to the third assessment report of the Intergovernmental Panel on Climate Change*. Cambridge University Press, Cambridge, Unite Kingdom.
- [16] Houghton, J. T., Ding, Y. D. J. G., Griggs, D. J., Noguer, M., Van der Linden, P. J., Dai, X., ... & Johnson, C. A. (2001). *Climate Change 2001: The Scientific Basis*. The Press Syndicate of the University of Cambridge, Cambridge, Unite Kingdom.
- [17] Rodenhouse, N. L., Matthews, S. N., McFarland, K. P., Lambert, J. D., Iverson, L. R., Prasad, A., Sillett, T. S., & Holmes, R. T. (2008). Potential effects of climate change on birds of the Northeast. *Mitigation and Adaptation Strategies for Global Change*, 13(5–6), 517–540. doi:10.1007/s11027-007-9126-1.
- [18] Contessa, G. M., Guardati, M., D'Arienzo, M., Poggi, C., Sandri, S., D'Auria, M. C., Genovese, E., & Cannatà, V. (2018). The impact of climate change on radiological practices in Italy. *The European Physical Journal Plus*, 133(9). doi:10.1140/epjp/i2018-12243-3.
- [19] Edwards, M., Johns, D. G., Licandro, P., John, A. W., & Stevens, D. P. (2008). *Ecological Status Report: Results from the CPR Survey 2006/2007*. SAHFOS Technical Report, 5, Plymouth, United Kingdom.
- [20] Worm, B., & Lotze, H. K. (2021). Marine biodiversity and climate change. *Climate Change: Observed Impacts on Planet Earth* (3rd Ed.), 2021, 445–464, Elsevier, Amsterdam, Netherlands. doi:10.1016/B978-0-12-821575-3.00021-9.
- [21] Din, A., Li, Y., Khan, T., & Zaman, G. (2020). Mathematical analysis of spread and control of the novel corona virus (COVID-19) in China. *Chaos, Solitons and Fractals*, 141(110286). doi:10.1016/j.chaos.2020.110286.

- [22] Khan, F. M., Khan, Z. U., Lv, Y. P., Yusuf, A., & Din, A. (2021). Investigating of fractional order dengue epidemic model with ABC operator. *Results in Physics*, 24(103510). doi:10.1016/j.rinp.2021.104075.
- [23] Ghanbari, B., & Atangana, A. (2020). A new application of fractional Atangana–Baleanu derivatives: Designing ABC-fractional masks in image processing. *Physica A: Statistical Mechanics and Its Applications*, 542, 123516. doi:10.1016/j.physa.2019.123516.
- [24] Din, A., Li, Y., & Liu, Q. (2020). Viral dynamics and control of hepatitis B virus (HBV) using an epidemic model. *Alexandria Engineering Journal*, 59(2), 667–679. doi:10.1016/j.aej.2020.01.034.
- [25] Younis, M., Seadawy, A. R., Baber, M. Z., Husain, S., Iqbal, M. S., R. Rizvi, S. T., & Baleanu, D. (2021). Analytical optical soliton solutions of the Schrödinger-Poisson dynamical system. *Results in Physics*, 27(104369). doi:10.1016/j.rinp.2021.104369.
- [26] Sabatier, J. A. T. M. J., Agrawal, O. P., & Machado, J. T. (2007). *Advances in fractional calculus*. Springer, Dordrecht, Netherlands. doi:10.1007/978-1-4020-6042-7.
- [27] Caputo, M., & Fabrizio, M. (2015). A new definition of fractional derivative without singular kernel. *Progress in Fractional Differentiation and Applications*, 1(2), 73–85. doi:10.12785/pfda/010201.
- [28] Atangana, A., & Baleanu, D. (2016). New fractional derivatives with nonlocal and non-singular kernel: Theory and application to heat transfer model. *Thermal Science*, 20(2), 763–769. doi:10.2298/tsci160111018a.
- [29] Rahman, M. ur, Arfan, M., Shah, K., & Gómez-Aguilar, J. F. (2020). Investigating a nonlinear dynamical model of COVID-19 disease under fuzzy caputo, random and ABC fractional order derivative. *Chaos, Solitons and Fractals*, 140, 110232. doi:10.1016/j.chaos.2020.110232.
- [30] Kumar, T. S. (2021). Hybrid nanofluid slip flow and heat transfer over a stretching surface. *Partial Differential Equations in Applied Mathematics*, 4(100070). doi:10.1016/j.padiff.2021.100070.
- [31] Rahman, M. U., Arfan, M., Shah, Z., Kumam, P., & Shutaywi, M. (2021). Nonlinear fractional mathematical model of tuberculosis (TB) disease with incomplete treatment under Atangana - Baleanu derivative. *Alexandria Engineering Journal*, 60(3), 2845–2856. doi:10.1016/j.aej.2021.01.015.
- [32] Khan, M. A., & Atangana, A. (2020). Modeling the dynamics of novel coronavirus (2019-nCov) with fractional derivative. *Alexandria Engineering Journal*, 59(4), 2379–2389. doi:10.1016/j.aej.2020.02.033.
- [33] Liu, Y., Fan, E., Yin, B., & Li, H. (2020). Fast algorithm based on the novel approximation formula for the caputo - fabrizio fractional derivative. *AIMS Mathematics*, 5(3), 1729–1744. doi:10.3934/math.2020117.
- [34] Zhang, M., Liu, Y., & Li, H. (2019). High- order local discontinuous Galerkin method for a fractal mobile/immobile transport equation with the Caputo–Fabrizio fractional derivative. *Numerical Methods for Partial Differential Equations*, 35(4), 1588–1612. doi:10.1002/num.22366.
- [35] Soldatenko, S., Bogomolov, A., & Ronzhin, A. (2021). Mathematical Modelling of Climate Change and Variability in the Context of Outdoor Ergonomics. *Mathematics*, 9(22), 2920. doi:10.3390/math9222920.
- [36] North, G. R. (1975). Analytical Solution to a Simple Climate Model with Diffusive Heat Transport. *Journal of the Atmospheric Sciences*, 32(7), 1301–1307. doi:10.1175/1520-0469(1975)032<1301:ASTASC>2.0.CO;2.
- [37] Budyko, M. I. (1969). The effect of solar radiation variations on the climate of the Earth. *Tellus A: Dynamic Meteorology and Oceanography*, 21(5), 611. doi:10.3402/tellusa.v21i5.10109.
- [38] Sellers, W. D. (1969). A global climatic model based on the energy balance of the earth-atmosphere system. *Journal of Applied Meteorology and Climatology*, 8(3), 392–400. doi:10.1175/1520-0450(1969)008<0392:AGCMBO>2.0.CO;2.
- [39] Podlubny, I. (1999). *Fractional differential equations, mathematics in science and engineering*. Academic Press, New York, United States.
- [40] Nawaz, Y., Arif, M. S., & Shatanawi, W. (2022). A New Numerical Scheme for Time Fractional Diffusive SEAIR Model with Non-Linear Incidence Rate: An Application to Computational Biology. *Fractal and Fractional*, 6(2), 78. doi:10.3390/fractalfract6020078.
- [41] Nawaz, Y., Arif, M. S., Shatanawi, W., & Ashraf, M. U. (2022). A new unconditionally stable implicit numerical scheme for fractional diffusive epidemic model. *AIMS Mathematics*, 7(8), 14299–14322. doi:10.3934/math.2022788.
- [42] Arif, M. S., Abodayeh, K., & Nawaz, Y. (2022). A Computational Approach to a Mathematical Model of Climate Change Using Heat Sources and Diffusion. *Civil Engineering Journal (Iran)*, 8(7), 1358–1368. doi:10.28991/CEJ-2022-08-07-04.
- [43] Nawaz, Y., Arif, M. S., Abodayeh, K., & Bibi, M. (2022). Finite difference schemes for time-dependent convection q-diffusion problem. *AIMS Mathematics*, 7(9), 16407–16421. doi:10.3934/math.2022897.